

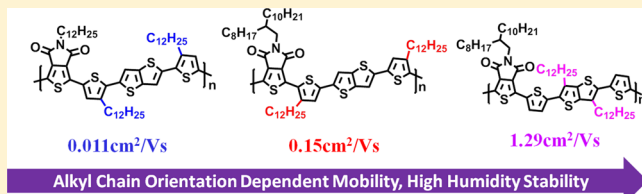
Thieno[3,4-*c*]pyrrole-4,6-dione Containing Copolymers for High Performance Field-Effect Transistors

Qinghe Wu, Mao Wang, Xiaolan Qiao, Yu Xiong, Yangguang Huang, Xike Gao, and Hongxiang Li*

Shanghai Institute of Organic Chemistry, Chinese Academy of Sciences, Shanghai 200032, China

Supporting Information

ABSTRACT: Thieno[3,4-*c*]pyrrole-4,6-dione (TPD) containing copolymer semiconductors P1–P3 were strategically designed and successfully synthesized. Their physicochemical properties were thoroughly investigated. All polymers exhibited good solution processability and high humidity stability in thin film transistors (TFTs). Transistor electrical characterization showed the device performance was sensitive to the alkyl chain substituent orientations of the polymers. A maximum TFT hole mobility of $\sim 1.29 \text{ cm}^2/(\text{Vs})$ was observed for P3-based devices, a recorded mobility for TPD containing polymer semiconductors reported to date. The corresponding thin-film morphologies and polymer chains packing were investigated in detail by AFM and 2D-GIXD to correlate with the alkyl orientation-dependent carrier mobility of P1–P3. Experimental results showed the alkyl chain orientations determined the polymer chains packing pattern in the thin films, the film morphologies, and the resulting device performances of P1–P3.



1. INTRODUCTION

Conjugation polymer semiconductors, as the active layer for large-area and low-cost organic thin-film transistors, have attracted intensive attention because of their intrinsic properties of mechanical flexibility, thermal stability, film uniformity, and solution processability.^{1–4} The common strategy for the design of high-performance polymer semiconductors is introducing new and/or different conjugation units such as diketopyrrolopyrrole (DPP),^{5–12} benzothiadiazole (BT),^{13–15} and thieno[3,2-*b*]thiophene (TT)^{7,16,17} into polymer backbones. Comparing with the efforts to develop new conjugation building blocks, to pursue high performance polymer semiconductors by changing the alkyl chain substituents is an efficient and cost-effective method. For example, the performance of the isoindigo-based polymers (chemical structures see Scheme 1) was tremendously improved while introducing the siloxane terminated groups and changing the branching point of the branched alkyl chains.^{18,19} The mobility of PDVT-10 (chemical structure see Scheme 1) was 2 times higher than that of PDVT-8, in which the alkyl chain substituents were 2-decyldodecyl and 2-octyldodecyl, respectively.²⁰

Until now, the efforts to change alkyl chain substituents are mainly focused on alkyl chains bulkiness,^{18,19,21} length,^{20,22} and substitution density,^{7,23–26} which has provided useful information for the rational design of high-performance polymer semiconductors. Other factors, such as the alkyl chain orientations, are rarely investigated. Though some pioneering works on the effect of alkyl orientations to polymer semiconductor's performance have been done,^{27,28} the details of the polymer packing patterns in solid state and how the orientation of alkyl chains affecting the polymer packing were not studied. Herein a deep investigation on this issue was

carried out; experimental results showed the alkyl chain orientations strongly affected the molecular packing pattern and the device performance.

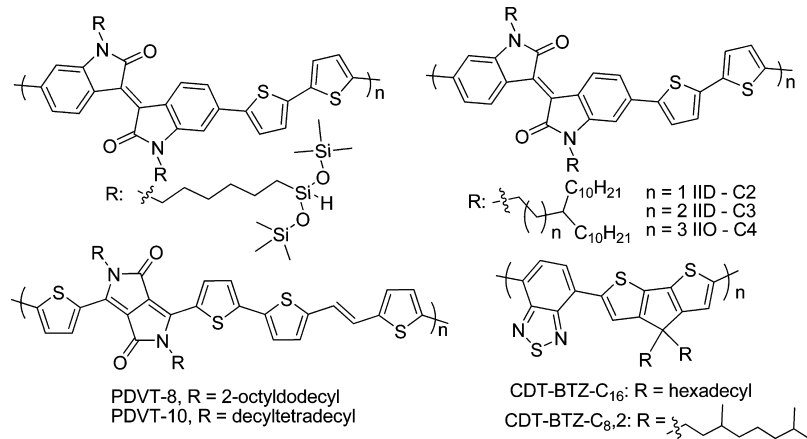
Thieno[3,4-*c*]pyrrole-4,6-dione (TPD), as an electron-deficient unit, has been used in low bandgap copolymers, which exhibited excellent power conversion efficiencies (3–7%) in photovoltaic devices.^{29–44} However, these polymers usually displayed low field-effect transistor performance (mobility below $0.01 \text{ cm}^2 \text{ V}^{-1} \text{ s}^{-1}$).^{31–33} Until now, the recorded mobility of TPD-contained polymers was $0.59 \text{ cm}^2 \text{ V}^{-1} \text{ s}^{-1}$, which was reported by Guo et al. and composed by TPD and oligo-thiophene units.²⁸ In this paper, TPD containing polymer semiconductors P1–P3 (chemical structure see Scheme 2), as an alkyl orientation design paradigm, were strategically design and successfully synthesized with the aim to (i) obtain high performance TPD-based polymer semiconductors and (ii) investigate the impact of the alkyl chains orientation on the polymer chains packing patterns in the solid state and the corresponding thin film transistor (TFT) performance. Possessing the interactions between TPD (the oxygen atom in carbonyl group) and adjacent thiophene (the sulfur in thiophene),⁴⁵ and the enlarged coplanar unit thieno[3,2-*b*]thiophene (TT),¹⁶ a maximum thin film transistor hole mobility of $1.29 \text{ cm}^2 \text{ V}^{-1} \text{ s}^{-1}$ was observed for P3-based devices, 2 times higher than the recorded mobility of TPD-containing polymers. Currently, all the reported polymer semiconductors with the carrier mobility above $2.0 \text{ cm}^2 \text{ V}^{-1} \text{ s}^{-1}$ have the number-average molecular weights (M_n) higher

Received: March 14, 2013

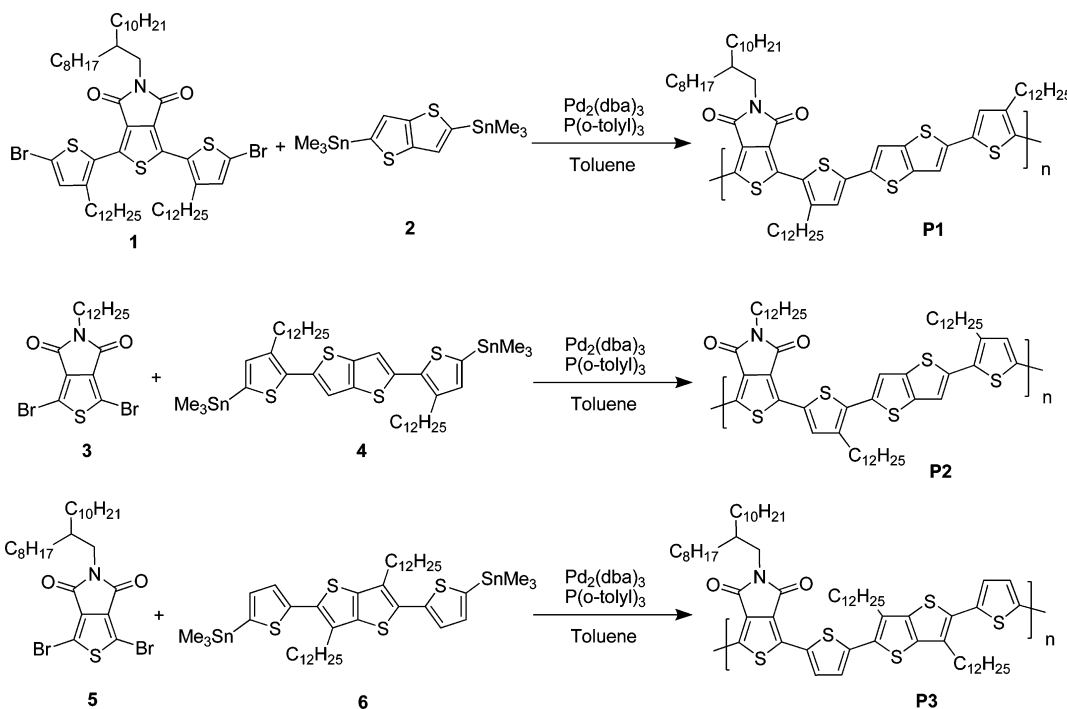
Revised: April 25, 2013

Published: May 7, 2013

Scheme 1. Chemical Structures of Some Reported High Performance Polymer Semiconductors



Scheme 2. Synthetic Routes and Chemical Structures of P1, P2, and P3



than 35 kDa and some of them even above 100 kDa (the molecular weight of polymers has great influence on the performance of polymer transistors);^{12,14,18–20} the hole mobility of $1.29 \text{ cm}^2 \text{ V}^{-1} \text{ s}^{-1}$ for **P3** with a M_n of 16 kDa is one of the highest values reported for polymer semiconductors. Moreover, **P1–P3** displayed strong alkyl chain substituent-dependent mobility. The mobility of **P3** is 1 and 2 orders of magnitude higher than those of **P1** and **P2**, which demonstrated a great influence of alkyl chain orientations on polymer transistors' performance and the efficacy of alkyl orientation design paradigm toward high performance polymer semiconductors. The effects of alkyl chain substituents to the polymer packing patterns, the film morphologies, and the intermolecular interactions in the solid state of **P1–P3** were investigated in detail by atomic force microscopy (AFM) and two-dimensional grazing incidence X-ray diffraction (2D-GIXD) spectrometry.

2. EXPERIMENTAL SECTION

2.1. General. All of the chemicals and solvents were used as received. Compounds **1–6** were synthesized according to the literature.^{28,46,47} ¹H NMR (300 MHz) spectra were measured in CDCl₂CDCl₂ on Varian Mercury (300 MHz) instruments, using tetramethylsilane as an internal standard. Elemental analyses were performed on an Elementar Vario EL III elemental analyzer. Molecular weights (M_n) and molecular weight distributions (PDI) for **P2** were measured at 40 °C on standard polystyrene (PS) gel permeation chromatography system equipped with a Waters 1515 isocratic HPLC pump, a Waters 2414 refractive index detector, and a set of Waters Styragel columns (HR3, HR4, and HR5, 7.8 × 300 mm), using tetrahydronfuran (THF) as the eluent at a flow rate of 1.00 mL/min. The M_n and PDI for **P1** and **P3** were recorded on a Polymer Laboratories GPC 220 instrument at 150 °C using standard polystyrene (PS) as the reference and 1,2,4-trichlorobenzene as the eluent at a flow rate of 1.00 mL/min. Absorption spectra were measured on a U-3900 UV-vis spectrophotometer. Cyclic voltammetric measurements were carried out in a conventional three-electrode cell using a platinum working electrode, a platinum wire

counter electrode, and a saturated calomel electrode (SCE) reference electrode on a computer-controlled CHI610D instrument. Atomic force microscopy (AFM) was recorded on a Nanoscope IIIa AFM in tapping mode. TGA was conducted with a PerkinElmer Pyris 1 TGA and was carried out on approximately 6–8 mg film samples heated in flowing nitrogen at a heating rate of 10 °C/min.

2.2. Materials Syntheses. Polymer P1. An air-free 50 mL flask was charged with 1 (0.325 g, 0.298 mmol), 2 (0.139 g, 0.298 mmol), $\text{P}(o\text{-tolyl})_3$ (18 mg, 0.06 mmol), $\text{Pd}_2(\text{dba})_3$ (14 mg, 0.015 mmol), and anhydrous toluene (15 mL) under a nitrogen stream. The reaction was stirred at 100 °C for 60 h. After cooling to room temperature, the deep blue mixture was slowly dropped into 300 mL of methanol (containing 10 mL of concentrated hydrochloric acid) with vigorous stirring. After stirring for 2 h, the precipitate was filtered and extracted by the Soxhlet with methanol, acetone, hexane, dichloromethane, and chloroform each for 24 h. After final extraction with dichlorobenzene, the polymer solution was concentrated to ~20 mL and then dropped into 200 mL of methanol with vigorous stirring. The polymer was collected by filtration and dried under reduced pressure to afford the product (0.265 g, 81.3%). Molecular weight (M_n) = 154 kDa; polydispersity (PDI) = 4.99. ^1H NMR (300 MHz, $\text{CDCl}_3/\text{CDCl}_2$) 0.80 (Br, 12H), 1.20 (Br, 68H), 1.64 (Br, 4H), 1.84 (Br, 1H), 2.75 (Br, 4H), 3.46 (Br, 2H), 7.07 (Br, 2H), 7.29 (Br, 2H). Anal. Calcd for $\text{C}_{64}\text{H}_{97}\text{NO}_2\text{S}_5$: C, 71.97; H, 8.94; N, 1.31%. Found: C, 71.65; H, 9.10; N, 1.12%.

Polymer P2. An air-free 50 mL flask was charged with 3 (0.183 g, 0.383 mmol), 4 (0.370 g, 0.383 mmol), $\text{P}(o\text{-tolyl})_3$ (23 mg, 0.08 mmol), $\text{Pd}_2(\text{dba})_3$ (18 mg, 0.020 mmol), and anhydrous toluene (15 mL) under a nitrogen stream. The reaction mixture was stirred at 100 °C for 60 h. After cooling to room temperature, the deep red mixture was slowly dropped into 300 mL of methanol (containing 10 mL of concentrated hydrochloric acid) with vigorous stirring. After stirring for 2 h, the precipitate was filtered and extracted by the Soxhlet with methanol, acetone, and hexane each for 24 h. After final extraction with dichloromethane, the polymer solution was concentrated to ~20 mL and then dropped into 200 mL of methanol with vigorous stirring. The polymer was collected by filtration and dried under reduced pressure to afford the product (0.060 g, 16.0%). M_n = 10.5 kDa, PDI = 1.2. ^1H NMR (300 MHz, $\text{CDCl}_3/\text{CDCl}_2$) 0.80 (Br, 9H), 1.26 (Br, 54H), 1.58 (Br, 6H), 2.76 (Br, 4H), 3.67 (Br, 2H), 7.16 (Br, 2H), 7.79 (Br, 2H). Anal. Calcd for $\text{C}_{56}\text{H}_{81}\text{NO}_2\text{S}_5$: C, 70.17; H, 8.31; N, 1.46%. Found: C, 69.96; H, 8.24; N, 1.23%.

Polymer P3. An air-free 50 mL flask was charged with 5 (0.182 g, 0.307 mmol), 6 (0.297 g, 0.307 mmol), $\text{P}(o\text{-tolyl})_3$ (19 mg, 0.062 mmol), $\text{Pd}_2(\text{dba})_3$ (14 mg, 0.015 mmol), and anhydrous toluene (15 mL) under a nitrogen stream. The reaction was stirred at 100 °C for 60 h. After cooling to room temperature, the deep blue mixture was slowly dropped into 300 mL of methanol (containing 10 mL of concentrated hydrochloric acid) with vigorous stirring. After stirring for 2 h, the precipitate was filtered and extracted by the Soxhlet with methanol, acetone, hexane, dichloromethane, and chloroform each for 24 h. After final extraction with dichlorobenzene, the polymer solution was concentrated to ~20 mL and then dropped into 200 mL of methanol with vigorous stirring. The polymer was collected by filtration and dried under reduced pressure to afford the product (0.19 g, 57.8%). M_n = 16 kDa, PDI = 2.06. ^1H NMR (300 MHz, $\text{CDCl}_3/\text{CDCl}_2$) 0.80 (Br, 12H), 1.20 (Br, 68H), 1.74 (Br, 4H), 1.89 (Br, 1H), 2.87 (Br, 4H), 3.52 (Br, 2H), 7.13 (Br, 2H), 7.99 (Br, 2H). Anal. Calcd for $\text{C}_{64}\text{H}_{97}\text{NO}_2\text{S}_5$: C, 71.97; H, 8.94; N, 1.31%. Found: C, 71.78; H, 8.94; N, 1.17%.

2.3. Thin Film Transistor Fabrication and Characterization. The devices are top-contact bottom-gate structure. The gate is n-type heavily doped Si. A thermally grown SiO_2 layer of 300 nm (the specific capacitance was measured to be 10 nF cm⁻²) is used as the gate dielectric layer. Thin films of P1, P2, and P3 were prepared by spin-coating the corresponding polymer solutions (4 mg/mL in 1,1,2,2-tetrachloroethane) on octadecyltrichlorosilane (OTS)-treated SiO_2/Si wafers. Au source and drain electrodes were deposited by vacuum evaporation on the top of the organic film through a shadow mask. The resulting device had a channel length of 31 μm and a width of 273 μm . Electrical measurements were carried out at room temperature in

air using a Keithley 4200 semiconductor parameter analyzer. The field-effect mobility and the threshold voltage (V_{TH}) were calculated by fitting a straight line to the plot of the square root of I_{DS} vs V_G (saturation region) according to the expression $I_{\text{DS}} = (W/2L)\mu_e C_i(V_G - V_{\text{TH}})^2$, where I_{DS} is the drain-source current, μ is the field-effect mobility, W is the channel width, L is the channel length, C_i is the capacitance per unit area of the gate dielectric layer, and V_{TH} is the threshold voltage.

3. RESULTS AND DISCUSSION

3.1. Synthesis and Physicochemical Properties. The chemical structures and synthetic route of polymers P1–P3 are shown in Scheme 2. All polymers have the same conjugation backbones but with different alkyl chain orientations. With the aim to increase the solubility, the nitrogen atoms of TPD units in P1 and P3 are substituted by branched alkyl chains. The polymers P2 and P3 were synthesized by conventional Stille coupling reaction between dibromo-TPD and the corresponding oligothiophene stanny regents. The attempt to synthesize the stanny regent of 2,5-bis(5-bromo-4-dodecylthiophen-2-yl)thieno[3,2-*b*]thiophene was failed because of the long dodecyl substituents, and P1 was prepared by coupling of thieno[3,2-*b*]thiophene stanny regent 1 and 1,3-bis[5-bromo-3-dodecylthiophen-2-yl]-TPD 2. P2 displays good solubility in common organic solvents; P1 and P3 are only soluble in hot chlorine-containing solvents such as chlorobenzene and 1,1,2,2-tetrachloroethane. The number-average molecular weights are 154 kDa (polydispersity (PDI) = 4.99) for P1, 10.5 kDa (PDI = 1.2) for P2, and 16 kDa (PDI = 2.06) for P3.

The absorption spectra of P1–P3 in 1,1,2,2-tetrachloroethane solution are shown in Figure 1. All of the solution

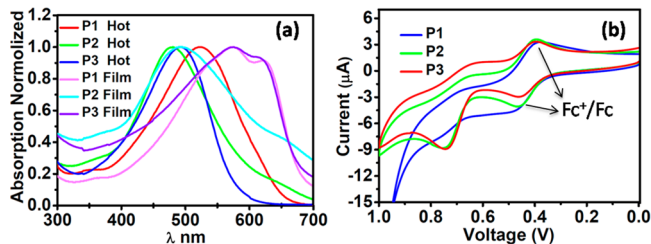


Figure 1. (a) UV-vis absorption spectra of P1, P2, and P3 in hot 1,1,2,2-tetrachloroethane solution (30 $\mu\text{g/mL}$) and on a quartz substrate (as deposited thin-film). (b) Cyclic voltammograms of the P1–P3 films on a platinum electrode. Bu_4NPF_6 was used as electrolyte, CH_3CN was used as solution, the scan rate was 50 mV s^{-1} , and ferrocene was used as internal standard.

absorption spectra were conducted at 80 °C due to the serious aggregations of polymers at room temperature. The maximum absorption (λ_{max}) for P1, P2, and P3 in solution are 525, 479, and 492 nm, respectively, which is congruent with the GPC data, indicating the variation is caused by the different conjugation length of P1–P3. Comparing with that of solutions, the maximum absorptions of P1 and P3 in the thin films are red-shifted 50 and 83 nm, respectively, and new shoulders at 625 and 620 nm are observed, suggesting the strong intermolecular interactions of P1 and P3 in the solid state. The absorption of P2 thin films becomes broad and the maximum absorption is slightly red-shifted compared with that of solution, indicating the lack of efficient intermolecular interactions in the thin films. The electrochemical properties of P1–P3 were investigated as thin films through cyclic voltammetry (CV), and the ferrocene/ferrocium (Fc/Fc^+)

was used as internal standard. All polymers display a quasi-reversible oxidation process with redox potentials located at 0.68–0.71 V. The highest occupied molecular orbits (HOMO) levels calculated from CV are −5.07 eV for **P1**, −5.06 eV for **P2**, and −5.05 eV for **P3**, which are lower than that of regioregular poly(3-hexylthiophene) (−4.76 eV)⁴⁸ and ∼0.3 eV higher than that of the polymers comprising TPD and oligotetrathiophene building units.²⁸ The HOMO energy levels of **P1–P3** have good match with the Fermi level of Au and will facilitate the hole injection from a gold source electrode to polymer layers.

3.2. Thin Film Transistors Characterization. The charge transport properties of the polymer **P1–P3** were investigated by thin film transistors. The transistors were fabricated with top-contact/bottom-gate device configurations. The polymers were spin-coated (4 mg/mL in 1,1,2,2-tetrachloroethane) on octadecyltrichlorosilane (OTS)-treated SiO₂/Si (300 nm) substrates. The Au source and drain electrodes were deposited through a shadow mask by vacuum evaporation, which gave a channel length of 31 μm and a width of 173 μm. All the devices were measured under ambient conditions. The mobility and threshold voltage were calculated from the saturation regimes. The transistor performances are collected in Table 1, and the

Table 1. TFT Characteristics of the Solution Processed Devices Based on **P1–P3**

polymers	$T_{\text{anneal}}^{\text{a}}$ (°C)	μ (cm ² V ^{−1} s ^{−1})	$I_{\text{on/off}}$	V_{th} (V)
P1	as deposited	0.055–0.097	$10^{4\text{--}5}$	−23 to −16
	230	0.11–0.15	$10^{4\text{--}5}$	−24 to −15
P2	as deposited	$(1.45\text{--}2.25) \times 10^{-5}$	10^2	−15 to −5
	230	$(4.30\text{--}11) \times 10^{-3}$	10^3	−30 to −10
P3	as deposited	0.020–0.029	$10^{4\text{--}5}$	−24 to −18
	260	0.90–1.29	$10^{6\text{--}7}$	−15 to −5

^aAnnealing temperatures given in this table were those that gave the best device performance.

representative transfer and output plots are shown in Figure 2. The as-deposited thin films of **P1** exhibited moderate transistor performance (mobility: 0.055–0.097 cm² V^{−1} s^{−1}). With thermal annealing, the mobility of **P1** thin films was slightly increased, and the highest mobility could reach 0.15 cm² V^{−1} s^{−1} after thermal annealing at 230 °C. The thin films of **P2** displayed the lowest mobility among the three polymers with a highest hole mobility of 1.1×10^{-2} cm² V^{−1} s^{−1} after thermal annealing. The as-deposited thin films of **P3** showed a mobility of 0.02–0.029 cm² V^{−1} s^{−1}. After thermal annealing at 230 °C, the transistor performance of **P3** was improved to 0.51–0.72 cm² V^{−1} s^{−1}. After further annealing at 260 °C, a highest mobility up to 1.29 cm² V^{−1} s^{−1} with average mobility of 1.04 cm² V^{−1} s^{−1} based on at least 20 devices was observed.

The polymer semiconductors with high molecular weight usually display high transistor performance compared with that of the lower ones, which has been well demonstrated for regioregular P3HT and CDT-BTZ copolymer.^{14,48,49} For example, the mobility of CDT-BTZ-C₁₆ (chemical structure see Scheme 1) is tremendously increased from 0.59 to 3.3 cm² V^{−1} s^{−1} when the M_n is improved from 16 to 35 kDa. Currently, to the best of our knowledge, all the reported polymer semiconductors with the carrier mobility above 2.0 cm² V^{−1} s^{−1}

have the M_n larger than 35 kDa and some of them even above 100 kDa.^{12,14,18–20} The mobility (1.29 cm² V^{−1} s^{−1}) for **P3** with a M_n of 16 kDa is one of the highest value reported for polymer semiconductors, suggesting TPD is a very promising building block for polymer semiconductors.

The wide variation in the mobility of **P1–P3** could not be ascribed to the molecular weight difference, since (i) **P1** possesses the highest molecular weight, but displays moderate charge carrier mobility, and (ii) the mobility of **P3** is about 2 orders of magnitude higher than that of **P2** while their molecular weights are slightly different. Therefore, there should be other factors accounting for the mobility variation of **P1–P3**.

3.3. Thin-Film Morphologies and Ordering Structures.

In order to deeply understand the mobility variation of **P1–P3**, the thin films morphology and the polymer packing in the thin films were studied by AFM and 2D-GIXD. The tapping mode AFM was employed to investigate the morphology of **P1–P3** thin films on OTS-modified SiO₂/Si substrates. As shown in Figure 3, the defined grains in the as-deposited **P1** thin film did not enlarge in size upon annealing at 230 °C, which was well correlated with the insensitivity of the transistor performance to thermal annealing. The obvious cracks in the as-deposited thin films of **P2** implied the poor continuity of the thin film. Upon annealing at 230 °C, nanorods with random orientation and large grain boundary were clearly observed in the **P2** thin films. The as-deposited thin films of **P3** displayed smooth and continuous featureless morphology. Upon thermal annealing at 260 °C, continuous thin films with intertwined nanorods were shown in the **P3** thin films, which provided efficient channels for the carrier transport. Additionally, small holes with size from several to tens of nanometers in diameter existed in the thermally annealed **P3** thin films, which exerted a negative effect on the device performance⁸ and suggested the device performance of **P3** could be further improved through the optimization of film deposition procedure.

2D-GIXD was carried out to probe the packing behaviors of **P1–P3** in their optimum films (Figure 4). All three polymers displayed successive diffraction features in the q_z -axis, indicating the formation of the layer-by-layer lamellar structures with the polymer backbones perpendicular to the substrate in the films. The interlayer distances calculated from the corresponding diffraction peaks (100) are 24.66 Å for **P1** and 24.31 Å for **P3**. These distances are much shorter than that of fully extended alkyl side chains (~36 Å), indicating that the side chains of **P1** and **P3** are strongly interdigitated among adjacent layers in the films. In contrast, the interlayer distance of **P2** is 34.1 Å, much larger than those of **P1** and **P3** and close to the length of fully extended alkyl chains, suggesting there are weak or even no alkyl chain interdigitations among adjacent layers. The lack of alkyl chain interdigitation might account for the film crack and large grain boundary of **P2**. The arc shape reflections in **P1** thin films and the spot reflections in **P2** thin films imply a small population of polymers adopts tilted orientations as well as face-on packing on the substrates.⁴⁹

All polymers showed π – π interactions in the films as evidenced by the in-plane diffraction peaks at 1.73, 1.71, and 1.68 Å^{−1}. The π – π stacking distances are 3.63 Å for **P1**, 3.67 Å for **P2**, and 3.74 Å for **P3**, short enough for the charge hopping between the adjacent polymer chains. The polymer semiconductors with short π – π stacking distance normally display higher carrier mobility.^{16,19,20} However, it is not the case for **P1–P3**. The **P3** with the best TFT performance possesses the

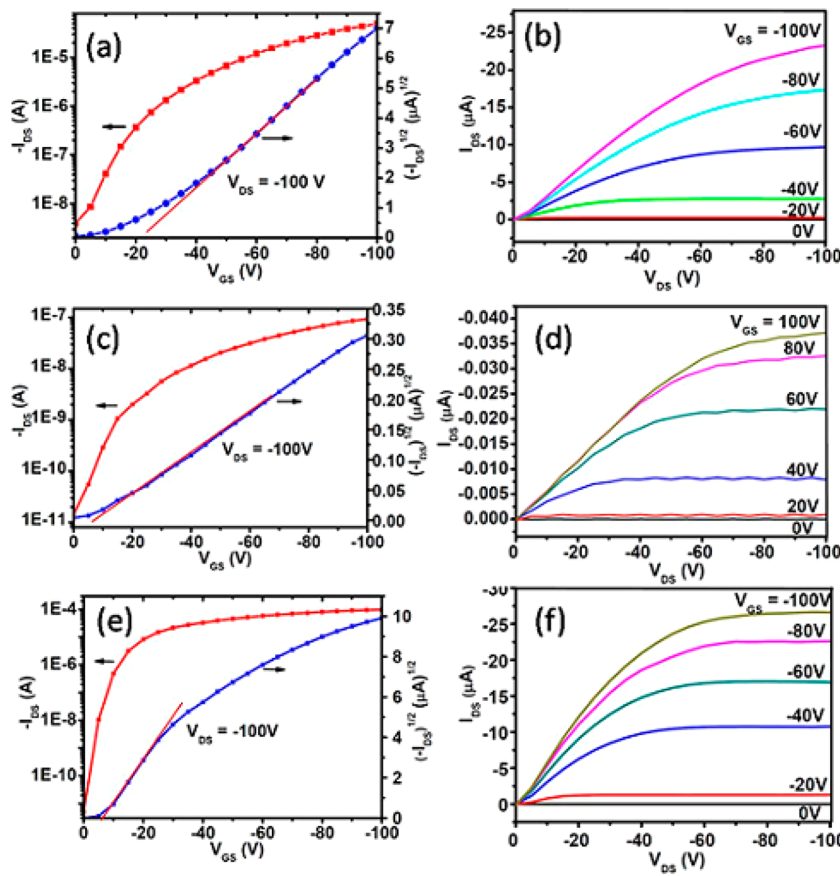


Figure 2. Typical transfer and output curves of P1–P3 thin film transistors: (a, b) P1; (c, d) P2; (e, f) P3.

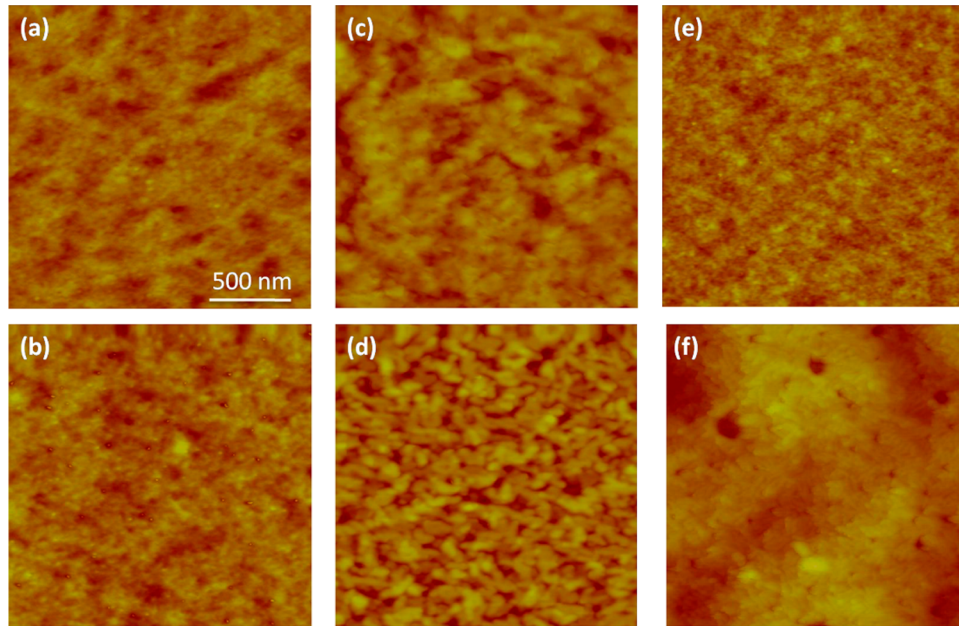


Figure 3. AFM images ($2 \times 2 \mu\text{m}$) of the thin films of P1–P3. P1: (a) as deposited, (b) annealed at 230°C ; P2: (c) as deposited, (d) annealed at 230°C ; P3: (e) as deposited, (f) annealed at 260°C .

longest $\pi-\pi$ stacking distance while P2 with the worst TFT performance has a moderate $\pi-\pi$ stacking distance. This may be ascribed to their different intermolecular overlaps evidenced by the thin films absorption spectra. We believe the interdigitations of alkyl chains, the efficient intermolecular interactions, the edge-on packing model of polymer chains on

substrate, and the high quality of the thin film should be jointly responsible for the high performance of P3.

3.4. Long-Range Alkyl Chains Structures and Correlations with Polymer Chains Stacking. The polymers P1–P3 possess the same π -conjugation backbone, and their plausible structures are illustrated in Figure 5.^{51,52} Though

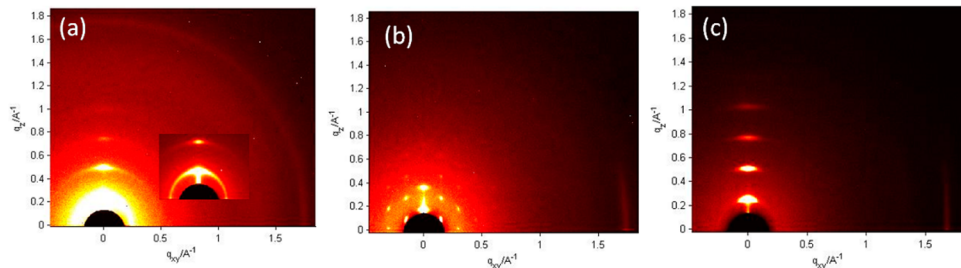


Figure 4. Two-dimensional grazing-incidence X-ray diffraction (2D-GIXD) spectra of **P1–P3** thin films: (a) **P1** (annealed at 230 °C); (b) **P2** (annealed at 230 °C); (c) **P3** (annealed at 260 °C).

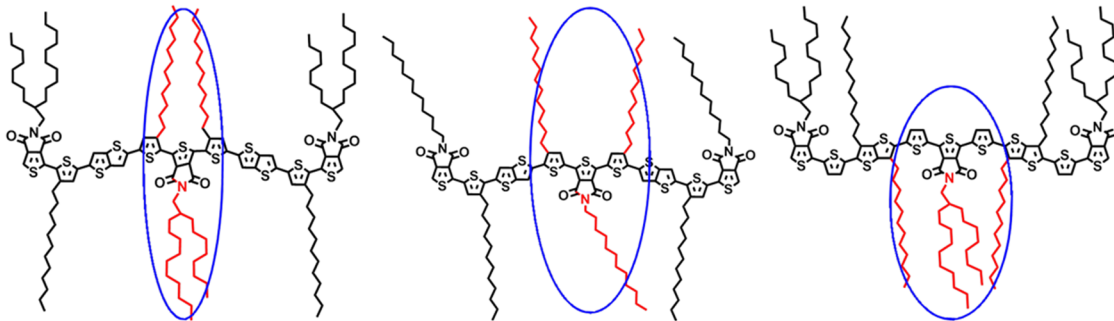


Figure 5. Optimized structures for polymers **P1**, **P2**, and **P3**. The alkyl chain clusters are marked by blue cycles.

P1–P3 have the same substituent density, their dissimilarity of the alkyl chain orientations in long range are too distinctive to ignore. The spaces between the clusters of the alkyl chains of **P1–P3**, as shown in Figure 5, have a sequence of **P3 > P1 > P2**. Moreover, **P1** and **P3** have better alkyl chain uniformity and symmetry than **P2**.

The large space between the clusters of the alkyl chains for **P3**, we believe, will facilitate the interdigitations of the side chains and the formation of lamellar stacking structures. Moreover, it favors large intermolecular overlaps, as indicated by the largest absorption red-shift of the thin films compared with that of solutions. The highly ordered lamellar packing with $\pi-\pi$ stacking and the large intermolecular overlap result in the excellent TFT performances of **P3**. The space between alkyl chain clusters of **P1** is not as large as that of **P3**, but the uniformity and the symmetry of the alkyl chains orientations guarantee the alkyl chain interdigitations and lamellar stacking in the thin films. The space between the alkyl chain clusters of **P2** is the smallest among the three polymers, and the alkyl chain orientation is not as uniform as that of **P1**, which hinders the interdigitations among alkyl chains and the efficient intermolecular overlaps in the solid state as evidenced by the solubility, the UV-vis absorption spectrum, and 2D-GIXD results. These results indicate the strong impact of the long-range alkyl chain orientations on the polymer packing in the solid state and the corresponding device performance.

3.5. Transistor Device Stability. Besides the high carrier mobility, the polymers displayed excellent environmental stability. The transistor performance of poly[2,5-di(thiophen-2-yl)thieno[3,2-*b*]thiophene] (**pBTTTs**), in which no TPD units were involved, decreased by a factor of 2 orders of magnitude when stored in ambient air (humidity level ~50%) for a week.¹⁶ **P1** and **P3** showed high ambient stability when stored at even higher humidity level ~60%. The mobility of **P1** decreased from 0.148 to 0.14 $\text{cm}^2 \text{V}^{-1} \text{s}^{-1}$ after 8 weeks storage, while the average mobility of **P3** based on nine devices

decreased from 1.09 to 0.95 $\text{cm}^2 \text{V}^{-1} \text{s}^{-1}$ after 13 weeks storage. To further investigate the stability of the polymers transistors under high humidity conditions, by using **P3** as an example, a drop of water was cast on the surface of the transistors for about 5 min, the water was wiped off, and the transistor was heated at 80 °C for 10 min; the mobility of the device was still above 0.3 $\text{cm}^2 \text{V}^{-1} \text{s}^{-1}$ (decreased from 0.99 to 0.34 $\text{cm}^2 \text{V}^{-1} \text{s}^{-1}$), demonstrating the excellent stability under high humidity conditions.

4. CONCLUSION

In summary, TPD-containing copolymers with the different alkyl chain orientation were strategically synthesized. These polymers displayed alkyl substituent-dependent hole mobility and excellent humidity stability. A highest mobility of 1.29 $\text{cm}^2 \text{V}^{-1} \text{s}^{-1}$ was observed for **P3**-based devices, a record value for TPD containing polymers reported to date. The mobilities of **P1** and **P2** were 0.15 and $1.1 \times 10^{-2} \text{ cm}^2 \text{V}^{-1} \text{s}^{-1}$, respectively. The corresponding thin-film morphologies and polymer chains packing were investigated in detail by AFM and 2D-GIXD to correlate with the alkyl orientation-dependent carrier mobility of **P1–P3**. 2D-GIXD results showed $\pi-\pi$ interactions were existed in all polymer thin films, and strong alkyl interdigitations were observed for the films of **P1** and **P3**. **P1–P3** formed ordered lamellar packing on the substrate, while a small population of tilted orientations as well as face-on packing was also observed for **P1** and **P2** thin films. The changes of packing models, intermolecular interactions, and film morphologies were caused by the difference of alkyl chain orientations of **P1–P3** in the long range. These results indicate the alkyl chain orientations (i) play crucial roles in the packing behavior of the polymer semiconductors in the solid state and eventually strongly influence the performance of the devices and (ii) should be paid more attention on rational design high performance polymer semiconductors.

■ ASSOCIATED CONTENT

Supporting Information

Thermogravimetric analysis, thin film XRD, and transistors operation stability. This material is available free of charge via the Internet at <http://pubs.acs.org>.

■ AUTHOR INFORMATION

Corresponding Author

*E-mail: lhx@mail.sioc.ac.cn (H.L.).

Notes

The authors declare no competing financial interest.

■ ACKNOWLEDGMENTS

This work was supported by the National Natural Sciences Foundation of China (21190031, 51273212) and the National Basic Research Program of China (2011CB808405). H. Li thanks the beamline BL14B1 (Shanghai Synchrotron Radiation Facility) for providing the beam time. We thank Prof. Jindong Zhang at Changchun Institute of Applied Chemistry, CAS, for the help with 2D-GIXD measurement.

■ REFERENCES

- (1) Bao, Z.; Dodabalapur, A.; Lovinger, A. J. *Appl. Phys. Lett.* **1996**, *69*, 4108.
- (2) Sirringhaus, H. *Adv. Mater.* **2005**, *17*, 2411.
- (3) Yan, H.; Chen, Z.; Zheng, Y.; Newman, C.; Quinn, J. R.; Dotz, F.; Kastler, M.; Facchetti, A. *Nature* **2009**, *457*, 679.
- (4) Beaujuge, P. M.; Frechet, J. M. *J. Am. Chem. Soc.* **2011**, *133*, 20009.
- (5) Chen, Z.; Lee, M. J.; Shahid Ashraf, R.; Gu, Y.; Albert-Seifried, S.; Meedom Nielsen, M.; Schroeder, B.; Anthopoulos, T. D.; Heeney, M.; McCulloch, I.; Sirringhaus, H. *Adv. Mater.* **2012**, *24*, 647.
- (6) Lee, J. S.; Son, S. K.; Song, S.; Kim, H.; Lee, D. R.; Kim, K.; Ko, M. J.; Choi, D. H.; Kim, B.; Cho, J. H. *Chem. Mater.* **2012**, *24*, 1316.
- (7) Bronstein, H.; Chen, Z.; Ashraf, R. S.; Zhang, W.; Du, J.; Durrant, J. R.; Tuladhar, P. S.; Song, K.; Watkins, S. E.; Geerts, Y.; Wienk, M. M.; Janssen, R. A.; Anthopoulos, T.; Sirringhaus, H.; Heeney, M.; McCulloch, I. *J. Am. Chem. Soc.* **2011**, *133*, 3272.
- (8) Li, Y.; Sonar, P.; Singh, S. P.; Soh, M. S.; van Meurs, M.; Tan, J. *J. Am. Chem. Soc.* **2011**, *133*, 2198.
- (9) Ha, J. S.; Kim, K. H.; Choi, D. H. *J. Am. Chem. Soc.* **2011**, *133*, 10364.
- (10) Kanimozhi, C.; Yaacobi-Gross, N.; Chou, K. W.; Amassian, A.; Anthopoulos, T. D.; Patil, S. *J. Am. Chem. Soc.* **2012**, *134*, 16532.
- (11) Wu, P. T.; Kim, F. S.; Jenekhe, S. A. *Chem. Mater.* **2011**, *23*, 4618.
- (12) Li, J.; Zhao, Y.; Tan, H. S.; Guo, Y.; Di, C. A.; Yu, G.; Liu, Y.; Lin, M.; Lim, S. H.; Zhou, Y.; Su, H.; Ong, B. S. *Sci. Rep.* **2012**, *2*, 754.
- (13) Osaka, I.; Shimawaki, M.; Mori, H.; Doi, I.; Miyazaki, E.; Koganezawa, T.; Takimiya, K. *J. Am. Chem. Soc.* **2012**, *134*, 3498.
- (14) Tsao, H. N.; Cho, D. M.; Park, I.; Hansen, M. R.; Mavrinskiy, A.; Yoon do, Y.; Graf, R.; Pisula, W.; Spiess, H. W.; Mullen, K. *J. Am. Chem. Soc.* **2011**, *133*, 2605.
- (15) Zhang, W.; Smith, J.; Watkins, S. E.; Gysel, R.; McGehee, M.; Salleo, A.; Kirkpatrick, J.; Ashraf, S.; Anthopoulos, T.; Heeney, M.; McCulloch, I. *J. Am. Chem. Soc.* **2010**, *132*, 11437.
- (16) McCulloch, I.; Heeney, M.; Bailey, C.; Genevicius, K.; Macdonald, I.; Shkunov, M.; Sparrowe, D.; Tierney, S.; Wagner, R.; Zhang, W.; Chabinyc, M. L.; Kline, R. J.; McGehee, M. D.; Toney, M. F. *Nat. Mater.* **2006**, *5*, 328.
- (17) Li, Y.; Singh, S. P.; Sonar, P. *Adv. Mater.* **2010**, *22*, 4862.
- (18) Mei, J.; Kim do, H.; Ayzner, A. L.; Toney, M. F.; Bao, Z. *J. Am. Chem. Soc.* **2011**, *133*, 20130.
- (19) Lei, T.; Dou, J.; Pei, J. *Adv. Mater.* **2012**, *24*, 6457.
- (20) Chen, H.; Guo, Y.; Yu, G.; Zhao, Y.; Zhang, J.; Gao, D.; Liu, H.; Liu, Y. *Adv. Mater.* **2012**, *24*, 4618.
- (21) Bao, Z. N.; Lovinger, A. J. *Chem. Mater.* **1999**, *11*, 2607.
- (22) Bronstein, H.; Leem, D. S.; Hamilton, R.; Woebkenberg, P.; King, S.; Zhang, W. M.; Ashraf, R. S.; Heeney, M.; Anthopoulos, T. D.; de Mello, J.; McCulloch, I. *Macromolecules* **2011**, *44*, 6649.
- (23) Kline, R. J.; DeLongchamp, D. M.; Fischer, D. A.; Lin, E. K.; Richter, L. J.; Chabinyc, M. L.; Toney, M. F.; Heeney, M.; McCulloch, I. *Macromolecules* **2007**, *40*, 7960.
- (24) Ong, B. S.; Wu, Y.; Li, Y.; Liu, P.; Pan, H. *Chem.—Eur. J.* **2008**, *14*, 4766.
- (25) Pan, H.; Wu, Y.; Li, Y.; Liu, P.; Ong, B. S.; Zhu, S.; Xu, G. *Adv. Funct. Mater.* **2007**, *17*, 3574.
- (26) Ong, B. S.; Wu, Y.; Liu, P.; Gardner, S. *J. Am. Chem. Soc.* **2004**, *126*, 3378.
- (27) Liu, J.; Zhang, R.; Sauve, G.; Kowalewski, T.; McCullough, R. D. *J. Am. Chem. Soc.* **2008**, *130*, 13167.
- (28) Guo, X.; Ortiz, R. P.; Zheng, Y.; Kim, M. G.; Zhang, S.; Hu, Y.; Lu, G.; Facchetti, A.; Marks, T. J. *J. Am. Chem. Soc.* **2011**, *133*, 13685.
- (29) Zou, Y.; Najari, A.; Berrouard, P.; Beaupre, S.; Aich, B. R.; Tao, Y.; Leclerc, M. *J. Am. Chem. Soc.* **2010**, *132*, 5330.
- (30) Piliego, C.; Holcombe, T. W.; Douglas, J. D.; Woo, C. H.; Beaujuge, P. M.; Frechet, J. M. *J. Am. Chem. Soc.* **2010**, *132*, 7595.
- (31) Guo, X. G.; Xin, H.; Kim, F. S.; Liyanage, A. D. T.; Jenekhe, S. A.; Watson, M. D. *Macromolecules* **2011**, *44*, 269.
- (32) Zhang, Y.; Zou, J. Y.; Yip, H. L.; Sun, Y.; Davies, J. A.; Chen, K. S.; Acton, O.; Jen, A. K. *J. Mater. Chem.* **2011**, *21*, 3895.
- (33) Hong, Y. R.; Wong, H. K.; Moh, L. C.; Tan, H. S.; Chen, Z. K. *Chem. Commun.* **2011**, *47*, 4920.
- (34) Zhang, Y.; Hau, S. K.; Yip, H. L.; Sun, Y.; Acton, O.; Jen, A. K. *Y. Chem. Mater.* **2010**, *22*, 2696.
- (35) Yuan, M. C.; Chiu, M. Y.; Liu, S. P.; Chen, C. M.; Wei, K. H. *Macromolecules* **2010**, *43*, 6936.
- (36) Griffini, G.; Douglas, J. D.; Piliego, C.; Holcombe, T. W.; Turri, S.; Frechet, J. M.; Mynar, J. L. *Adv. Mater.* **2011**, *23*, 1660.
- (37) Chu, T. Y.; Lu, J.; Beaupre, S.; Zhang, Y.; Pouliot, J. R.; Wakim, S.; Zhou, J.; Leclerc, M.; Li, Z.; Ding, J.; Tao, Y. *J. Am. Chem. Soc.* **2011**, *133*, 4250.
- (38) Najari, A.; Beaupre, S.; Berrouard, P.; Zou, Y. P.; Pouliot, J. R.; Lepage-Perusse, C.; Leclerc, M. *Adv. Funct. Mater.* **2011**, *21*, 718.
- (39) Zhang, G.; Fu, Y.; Zhang, Q.; Xie, Z. *Chem. Commun.* **2010**, *46*, 4997.
- (40) Chen, G. Y.; Cheng, Y. H.; Chou, Y. J.; Su, M. S.; Chen, C. M.; Wei, K. H. *Chem. Commun.* **2011**, *47*, 5064.
- (41) Braunecker, W. A.; Owczarczyk, Z. R.; Garcia, A.; Kopidakis, N.; Larsen, R. E.; Hammond, S. R.; Ginley, D. S.; Olson, D. C. *Chem. Mater.* **2012**, *24*, 1346.
- (42) Amb, C. M.; Chen, S.; Graham, K. R.; Subbiah, J.; Small, C. E.; So, F.; Reynolds, J. R. *J. Am. Chem. Soc.* **2011**, *133*, 10062.
- (43) Zhou, E. J.; Cong, J. Z.; Tajima, K.; Yang, C. H.; Hashimoto, K. *J. Phys. Chem. C* **2012**, *116*, 2608.
- (44) Gendron, D.; Morin, P. O.; Berrouard, P.; Allard, N.; Aich, B. R.; Garon, C. N.; Tao, Y.; Leclerc, M. *Macromolecules* **2011**, *44*, 7188.
- (45) Berrouard, P.; Grenier, F.; Pouliot, J. R.; Gagnon, E.; Tessier, C.; Leclerc, M. *Org. Lett.* **2011**, *13*, 38.
- (46) Li, Y.; Wu, Y.; Liu, P.; Birau, M.; Pan, H.; Ong, B. S. *Adv. Mater.* **2006**, *18*, 3029.
- (47) Mishra, S. P.; Palai, A. K.; Kumar, A.; Srivastava, R.; Kamalasan, M. N.; Patri, M. *Macromol. Chem. Phys.* **2010**, *211*, 1890.
- (48) Zhang, R.; Li, B.; Iovu, M. C.; Jeffries-El, M.; Sauve, G.; Cooper, J.; Jia, S.; Tristram-Nagle, S.; Smilgies, D. M.; Lambeth, D. N.; McCullough, R. D.; Kowalewski, T. J. *J. Am. Chem. Soc.* **2006**, *128*, 3480.
- (49) Kline, R. J.; McGehee, M. D.; Kadnikova, E. N.; Liu, J. S.; Frechet, J. M. *J. Adv. Mater.* **2003**, *15*, 1519.
- (50) Zhang, X.; Richter, L. J.; DeLongchamp, D. M.; Kline, R. J.; Hammond, M. R.; McCulloch, I.; Heeney, M.; Ashraf, R. S.; Smith, J. N.; Anthopoulos, T. D.; Schroeder, B.; Geerts, Y. H.; Fischer, D. A.; Toney, M. F. *J. Am. Chem. Soc.* **2011**, *133*, 15073.
- (51) Azumi, R.; Mena-Osteritz, E.; Boese, R.; Benet-Buchholz, J.; Bauerle, P. *J. Mater. Chem.* **2006**, *16*, 728.

(52) He, M.; Li, J.; Sorensen, M. L.; Zhang, F.; Hancock, R. R.; Fong, H. H.; Pozdin, V. A.; Smilgies, D. M.; Malliaras, G. G. *J. Am. Chem. Soc.* 2009, 131, 11930.